# Generation of Waves in the Concurrent Flow of Air and a Liquid

**LEONARD S. COHEN and THOMAS J. HANRATTY**

University of Illinois, Urbana, Illinois

**If air flows concurrently with a liquid, there are critical air velocities above which two-dimensional and three-dimensional waves appear at the interface. The physical process responsible for these transitions is as follows: The disturbance in the velocity field in the air caused by these waves gives rise to pressure and shear stress variations over the wavy surface. Pressure variations in phase with the wave slope and shear stress variations in phase with the wave height transmit energy from the air flow to the liquid film. If the rate at which energy is transmitted to the waves by these mechanisms is not larger than the rate of viscous dissipation in the liquid, the waves will decay.**

**The model of the gas flow proposed by Miles and Benjamin is used to calculate shear stress and pressure variations over the wavy surface. The agreement between predicted and measured critical air velocities, wave lengths, and wave velocities is good.**

If air is blown over a liquid, surface waves can be generated at the air-liquid interface. A knowledge of the physical processes responsible for the generation of these waves is needed if one is to understand many of the phenomena which are observed in two-phase flow systems. A study (*5, 7*) of the concurrent flow of air and water in a rectangular channel has revealed that at a constant liquid rate there is a critical air velocity above which waves will exist at the interface. The first disturbances which appear as the air velocity is increased are two-dimensional waves which extend over the whole width of the channel. At a higher gas velocity these two-dimensional waves change to a three-dimensional pebbled wave structure. This paper will present further experimental results and a theoretical interpretation of the transitions to two- and three-dimensional wave structures.

Ursell (*23*), in 1956, presented a critical review of work done on the generation of water waves. Since this review, important contributions to the problem have been made by Phillips (*21*) Miles (*14, 15, 16, 17, 18*), and Benjamin (*1*). Studies of the pressure variation over solid wavy surfaces have been presented by Motzfeld (*20*) and by Stanton, Marshall, and Houghton (*22*).

## EXPERIMENTS

Experiments were performed in a horizontal Plexiglas channel which was 12 in. wide, 1.015 in. high, and 21 ft. long. Details of the design of the system have been presented in previous publications (*5, 11*). Liquid flowed on the bottom of the channel, and gas flowed on top of the liquid concurrently with it. The liquid height varied from 0.07 to 0.3 in. The liquid was glycerine-water solutions whose viscosities varied from 2.0 to 27 lb./ft. hr. The liquid entered the channel through sixty 0.154-in. diameter holes which were slanted 45 deg. to the direction of flow. A 200-mesh copper screen lay over the perforated entry area preventing jetting of liquid at high flow rates. An artificial disturbance was created by inserting a 12 in. long, 0.1 in. high copper trip bar at the edge of the liquid entry area. The entry for the air consisted of a 2½ ft. long sheet metal adapter changing from a 7-in. circular cross section to a 12 × 1 in. rectangular cross section.

The disturbances artificially introduced into the liquid film are damped out at some distance downstream of the entry if the gas flow rate was below the critical value. The types of wave patterns that are observed are described in previous papers (*5, 6, 11*). If the trip bar was removed, the same types of wave structures were noted as existed with the trip bar. With no trip bar, the two-dimensional waves were first observed at the downstream end of the channel (*10*). Critical gas velocities were about 30% higher than were obtained with the trip bar. One would expect the observed transitions for the disturbed and undisturbed entry to be closer if a longer channel were used.

The transition from a two-dimensional wave regime to a three-dimensional wave regime was determined visually and by inspection of pressure drop data. The definition of this transition was more arbitrary than the definition of the two-dimensional transition, but it corresponded roughly to the appearance of waves whose characteristic lengths in the direction of flow and perpendicular to the direction of flow were equal.

The critical gas velocities increased with a decrease in the liquid height and an increase in the liquid viscosity. Hershman (*7*), who investigated a range of fluid viscosities from 2 to 32 lb./ft. hr., found that the critical gas velocity increased monotonically with decreasing liquid Reynolds number. The two-dimensional waves were found to be more stable the more viscous the solution. For water, three-dimensional waves appeared at only slightly higher gas velocities than are needed to generate two-dimensional waves. For the more viscous solutions, the two-dimensional waves were stable over a large range of gas flow rates.

The wave velocities were larger than the maximum liquid velocity but were much smaller than the average gas velocity.

A detailed summary of the experimental results is presented in a thesis by one of the authors (*3*).

## INTERPRETATION OF THE EXPERIMENTS

Since the wave velocity was always greater than the liquid velocity, it is apparent that the disturbances in the liquid film did not receive their energy from the average velocity profile of the liquid film. They were not the re-

Leonard S. Cohen is presently with United Aircraft, Hartford, Connecticut.

sult of a Tollmien-Schlichting instability in the liquid as described by Miles (*19*) and Feldman (*4*). It also appears that the waves are not the result of turbulent pressure fluctuations in the gas flow above the liquid surface. Smooth interfaces were observed in the presence of turbulent gas flows. Since the wave velocities were much smaller than the average gas velocity, a resonance mechanism of the type described by Phillips (*21*) could not be responsible for the generation of waves. Components of the turbulent pressure fluctuations with wave lengths comparable to those observed at the liquid interface would have velocities much larger than the wave velocities, since they would be comparable in magnitude to the average gas velocity.

It will be shown that the wave motion received its energy from pressure variations and shear stress variations at the interface resulting from gas flow fluctuations caused by the waves. The pressure variations transmit energy to the liquid through liquid velocity components in the vertical direction, while shear stress fluctuations transmit energy through liquid velocity components in the horizontal direction. Because of the small viscosity of air, shear stress variations are generally much smaller than the pressure variations. However, the wave motion on very thin films causes velocity fluctuations in the horizontal direction which are much larger than the velocity fluctuations in the vertical direction. Therefore, shear stress variations could be playing an important role in generating the waves observed in the experiments reported in this paper. The pressure variations in the gas over the wavy surface are assumed to be of the form

$$P' = \hat{P} \exp \{i(\alpha x + \beta z) - i\alpha C t\} \tag{1}$$

where

$$\hat{P} = \hat{P}_R + i\hat{P}_I \tag{2}$$

The shear stress variations are represented as

$$T' = \hat{T} \exp \{i(\alpha x + \beta z) - i\alpha C t\} \tag{3}$$

$$\hat{T} = \hat{T}_R + i\hat{T}_I \tag{4}$$

A sketch of the system that will be treated without waves at the interface is shown in Figure 1. The $x$ coordinate lies in the direction of mean flow, while the $y$ coordinate is in the vertical direction with $y = 0$ being located at the undisturbed interface. The average velocity in the liquid film will vary from zero at the wall to a value $\bar{u}_o$ at the interface. The air has a velocity $\bar{u}_o$ at the interface and a velocity of zero at the top wall. Measurements indicated that the maximum gas velocity was approximately at the center of the gas layer. Since the flow is fully developed, the average velocities in the gas and the liquid are not changing in the $x$ direction.

A small disturbance of the form

$$h' = \hat{h} \exp \{i(\alpha x + \beta z) - i\alpha C t\} \tag{5}$$

is introduced at the interface, and the conditions for which $C_I = 0$ are evaluated. This disturbance is accompanied by velocity and pressure fluctuations in the liquid film:

$$\frac{u'}{\hat{u}(y)} = \frac{v'}{\hat{v}(y)} = \frac{w'}{\hat{w}(y)} = \frac{h'}{\hat{h}(y)} = \frac{p'}{\hat{p}(y)} = \exp \{i(\alpha x + \beta z) - i\alpha C t\} \tag{6}$$

If Equations (6) are introduced into the equations of motion and second-order terms in the disturbances are neglected, the following relations are obtained for the fluctuating flow and the mean flow:

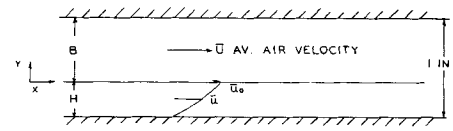


**Fig. 1. System to be analyzed.**

$$[D^2 - (\alpha^2 + \beta^2) - i\alpha N_{R_o} (\bar{u} - C)] \hat{u} = N_{R_o} \hat{v} (D\bar{u}) + i\alpha N_{R_o} \hat{p} - i\alpha \hat{h} N_F^{-2} N_{R_o} \tag{7}$$

$$[D^2 - (\alpha^2 + \beta^2) - i\alpha N_{R_o} (\bar{u} - C)] \hat{v} = N_{R_o} (D\hat{p}) \tag{8}$$

$$[D^2 - (\alpha^2 + \beta^2) - i\alpha N_{R_o} (\bar{u} - C)] \hat{w} = N_{R_o} i\beta \hat{p} - i\beta h N_F^{-2} N_{R_o} \tag{9}$$

$$i(\alpha \hat{u} + \beta \hat{w}) + D\hat{v} = 0 \tag{10}$$

$$\frac{1}{N_{R_o}} \frac{d^2\bar{u}}{dy^2} - \frac{\partial \bar{p}}{\partial x} = 0 \tag{11}$$

$$\frac{1}{N_F^2} + \frac{\partial \bar{p}}{\partial y} = 0 \tag{12}$$

$$\frac{\partial \bar{p}}{\partial z} = 0 \tag{13}$$

In Equations (1) to (13) the variables have been made dimensionless with respect to the liquid surface velocity $\bar{u}_o$ and the average film height $H$ and

$$N_{R_o} = \frac{\bar{u}_o H}{\nu} \tag{14}$$

$$N_F = \frac{\bar{u}_o}{\sqrt{gH}} \tag{15}$$

## TWO-DIMENSIONAL DISTURBANCES

If the disturbances at the interface are two-dimensional waves, $w = 0$ and $\beta = 0$, and (7), (8), and (10) yield the Orr-Sommerfeld equation:

$$\frac{1}{i\alpha^2 \mathcal{R}} [D^4 - 2\alpha^2 D^2 + \alpha^4] \hat{v} = \left(\frac{\bar{u}}{C} - 1\right)\left(\frac{D^2}{\alpha^2} - 1\right) v - \mathcal{L}\hat{v} \tag{16}$$

$$\mathcal{R} = \alpha C N_{R_o} \qquad \mathcal{L} = \frac{D^2\bar{u}}{C\alpha^2} \tag{17a, b}$$

Since the experiments indicate that waves are generated at large values of $\mathcal{R}$, solutions for (16) were sought for large values of this parameter. In this limit the viscous terms on the left side of (16) are negligible over most of the flow field, except for very thin viscous layers at the interface, at the bottom of the channel, and the critical point where $\bar{u} = C$. Since the wave velocities were always greater than the liquid velocity, a critical point did not exist in the liquid film, and only two viscous layers had to be considered. As is discussed by Lin (*12*), the four solutions of (16) for large $\mathcal{R}$ consist of two inviscid solutions obtained by neglecting the terms on the left side, a viscous solution which is significant only in the vicinity of the interface and another viscous solution which is significant only in the vicinity of the solid surface.

Since $|\mathcal{L}| << 1$, the inviscid solutions may be taken as

$$\hat{v}_1 = d_1 \exp(\alpha y) \tag{18}$$

$$\hat{v}_2 = d_2 \exp(-\alpha y) \tag{19}$$

The viscous solutions are obtained by a method outlined by Lock (13). The solution which is important near the wall is

$$\hat{v}_3 = d_3 e^{m\eta}\left[1 + \mathcal{R}^{-1/2}\left(-\frac{i5(D\bar{u})_w}{4Cm^2} + \frac{i(D\bar{u})_w\eta^2}{4Cm}\right) + \ldots\right] \tag{20}$$

$$\eta = (1+y)\,\mathcal{R}^{1/2} \tag{21}$$

$$m = \sqrt{-i} \tag{22}$$

The viscous solution which decays away from the interface is

$$\hat{v}_4 = d_4 e^{-s\xi}\left[1 - i\mathcal{R}^{-1/2}\left\{\frac{5(D\bar{u})_o}{4Cs^2}\xi + \frac{(D\bar{u})_o}{4Cs}\xi^2\right\} + \ldots\right] \tag{23}$$

$$\xi = y\,\mathcal{R}^{1/2} \tag{24}$$

$$s^2 = -i\left(\frac{C-1}{C}\right) \tag{25}$$

For the case of $h'$ being very small, the kinematic condition at the interface is

$$v'(0) = \frac{\partial h'}{\partial t} + \bar{u}_o\frac{\partial h'}{\partial x} \tag{26}$$

By substituting (6) into (26) and taking $\beta = 0$ and $\bar{u}_o = 1$, one obtains

$$\hat{h} = \frac{i\hat{v}(0)}{\alpha(C-1)} \tag{27}$$

the relation between the wave height amplitude and the disturbance velocity amplitude.

At the wall both the normal and the tangential velocity components vanish. This yields the condition that

$$\hat{u} = \hat{v} = 0 \qquad \text{at } y = -1 \tag{28}$$

The other two boundary conditions are obtained from a balance of the normal and shear stresses across the interface, with (1) and (3) used to represent the stresses imposed on the interface by the air flow.

Let $\tau_{x'y'}$, $\tau_{x'x'}$, and $\tau_{y'y'}$ be the stress components in the liquid for an $x' - y'$ coordinate system, in which $x'$ is measured along the wave surface and $y'$ is measured normal to the wave surface. Then for a two-dimensional wave structure

$$T = (\tau_{x'y'})_{y=h'} \tag{29}$$

$$-P = (\tau_{y'y'})_{y=h'} + N_W\frac{\partial^2 h'}{\partial x^2} \tag{30}$$

$$\tau_{x'x'} + \tau_{y'y'} = -2p \tag{31}$$

where

$$N_W = \frac{\sigma}{\rho\,\bar{u}_o^2 H} \tag{32}$$

The stress components in (29), (30), and (31) are transformed to an $x - y$ coordinate system in which $x$ is measured along the direction of the undisturbed interface, the slope of the waves are taken to be very small, and the second-order terms in the disturbances to the mean flow are neglected. There results

$$\bar{T} = N_{R_o}^{-1}(D\bar{u})_{y=h'} \tag{33}$$

$$T' = N_{R_o}^{-1}\left(\frac{\partial u'}{\partial y} + \frac{\partial v'}{\partial y}\right)_{y=h'} \tag{34}$$

Evaluating the right side of (34) at $y = 0$ and making use of (3), (6), (10), and (27), one obtains the boundary condition

$$D^2\hat{v} + \alpha^2\hat{v} - \frac{N_{R_o}\hat{T}\hat{v}}{\hat{h}(C-1)} = 0 \quad \text{at } y = 0 \tag{35}$$

The balance of the normal stress components represented by (30) may be transformed in a similar manner to yield

$$2\frac{\partial h'}{\partial x}\bar{T} + p' - P' + N_w\frac{\partial^2 h'}{\partial x^2} - 2N_{R_o}^{-1}\left(\frac{\partial v'}{\partial y}\right) = 0 \quad \text{at } y = 0 \tag{36}$$

If (36) is differentiated with respect to $x$ and combined with the equation of motion in the $x$-direction to eliminate $\partial p'/\partial x$, and if (1), (6), (10), and (27) are substituted into the resulting equation, the following boundary condition is obtained:

$$[D^2 - 3\alpha^2 - i\alpha N_{R_o}(\bar{u} - C)](D\hat{v}) + i\alpha N_{R_o}(D\bar{u})\hat{v} - \frac{2\hat{v}\,\alpha^2 N_{R_o}\bar{T}}{(C-1)} - \alpha^2 N_{R_o}\left[\frac{i\hat{v}\hat{P}}{\hat{h}\,\alpha(C-1)} + \frac{iN_w\alpha\hat{v}}{(C-1)} + \frac{i\hat{v}}{\alpha(C-1)N_F^2}\right] = 0 \quad \text{at } y = 0 \tag{37}$$

The complete solution of the Orr-Sommerfeld equation is a linear combination of the two viscous and two inviscid solutions:

$$\hat{v} = \sum_{j=1}^{4} d_j\hat{v}_j \tag{38}$$

In (38), $\hat{v}_1$, $\hat{v}_2$, $\hat{v}_3$, and $\hat{v}_4$ are given by (18), (19), (20), (23), and the constants $d_j$ are determined from the boundary conditions (28), (35), and (37). Four homogeneous equations in $d_j$ result, and a solution can exist only if the determinant of the coefficients of the $d_j$ vanishes.

The determinant is evaluated retaining the three highest orders in $\mathcal{R}$ and imposing the condition that the imaginary part of the wave velocity is zero. The imaginary part of the determinant yields a relation for the wave velocity:

$$C = 1 - \frac{(D\bar{u})_o}{2\alpha}\tanh\alpha \pm \left[\left(\frac{(D\bar{u})_o}{2\alpha}\tanh\alpha\right)^2 + \tanh\alpha\left(\alpha N_W + \frac{1}{\alpha N_F^2} + \frac{\hat{P}_R}{\alpha\hat{h}}\right)\right]^{1/2} \tag{39}$$

The wave velocity relative to the interface $(C - 1)$ predicted by (39) is the same as that given by Kelvin-Helmholtz theory (9), except that terms involving the velocity gradient at the surface appear in (39) and that $\hat{P}_R$ is left undefined.

The real part of the secular determinant yields the following condition for neutral stability:

$$\frac{\hat{P}_I}{\hat{h}} + \frac{\hat{T}_R}{\hat{h}}\left(\coth\alpha + \frac{(D\bar{u})_o}{\alpha(C-1)}\right) = \frac{4(D\bar{u})_o\alpha}{N_{R_o}} + \frac{4\alpha^2(C-1)\coth\alpha}{N_{R_o}} + \frac{\alpha^{3/2}(C-1)^2(\coth^2\alpha - 1)}{(2\,C\,N_{R_o})^{1/2}} \quad (40)$$

The term $\left(\coth\alpha + \frac{(D\bar{u})_o}{\alpha(C-1)}\right)$ multiplying the shear stress fluctuation amplitude equals the ratio $|\hat{u}(0)/\hat{v}(0)|$. If (40) is multiplied by $\hat{v}(0)$, the terms on the left side represent the energy transferred from the gas to the liquid by the pressure variations and shear stress variations over the wavy surface. Although $\hat{T}_R$ is expected to be much smaller than $\hat{P}_I$, the relative contribution of energy to the liquid by the shear stress variations can be significant if $\hat{u}(0) >> \hat{v}(0)$. This condition will be attained if the wave length is large compared with the liquid height. The first term on the right side of (40) is generally much smaller than the other two terms. The second and third terms on the right side of (40) are respectively measures of the viscous dissipation in the interface and at the wall. For wave lengths which are small compared with the film height, $(\coth^2\alpha - 1) \to 0$ and the viscous dissipation at the wall is not significant. Since $\alpha$ is inversely proportional to the wave length, the dissipation in the viscous layer at the interface becomes quite large for small wave lengths. For large wave lengths, the dissipation in the viscous layer at the wall is much larger than in the viscous layer at the interface since it is of higher order in the Reynolds number. Therefore, the waves first observed on the liquid film have a length of the same order as the liquid height. The wave lengths are small enough so the viscous dissipation in the wall layer is relatively unimportant; yet they are large enough so that dissipation in the viscous layer in the interface is not too great.

## THE GROWTH FACTOR

Small disturbances which appear at the air-liquid interface in a region of instability will initially increase exponentially with time [$\sim \exp(\alpha C_I t)$]. The growth factor $\alpha C_I$ can be evaluated from the determinant of the coefficients in (38) for the case of $C_R >> C_I$ and $C_I^2 \approx 0$ as

$$\alpha C_I = \left\{2(C_R-1)\coth\alpha + \frac{(D\bar{u})_o}{\alpha}\right\}^{-1} \left\{\frac{\hat{P}_i}{\hat{h}} + \frac{\hat{T}_R}{\hat{h}}\left(\coth\alpha + \frac{(D\bar{u})_o}{\alpha(C_R-1)}\right) - \frac{4\alpha(D\bar{u})_o}{N_{R_o}} - \frac{4\alpha^2(C_R-1)\coth\alpha}{N_{R_o}} - \frac{\alpha^{3/2}(C_R-1)^2(\coth^2\alpha-1)}{(2C_R\,N_{R_o})^{1/2}}\right\} \quad (41)$$

## THREE-DIMENSIONAL DISTURBANCES

The preceding results for two-dimensional waves may be extended to include three-dimensional waves by means of Squire's transformations *(12)*. The conditions for neutral stability for three-dimensional disturbances are

$$C = 1 - \frac{(D\bar{u})_o}{2\tilde{\alpha}}\tanh\tilde{\alpha} \pm \left\{\left(\frac{(D\bar{u})_o}{2\tilde{\alpha}}\tanh\tilde{\alpha}\right)^2 + \frac{\tilde{\alpha}\tanh\tilde{\alpha}}{\alpha^2}\left(\tilde{\alpha}^2 N_w + N_F^{-2} + \frac{\hat{P}_R}{\hat{h}}\right)\right\}^{1/2} \quad (42)$$

$$\frac{\hat{P}_I}{\tilde{\alpha}\hat{h}} + \frac{\hat{S}_R}{\tilde{\alpha}\hat{h}}\left(\coth\tilde{\alpha} + \frac{(D\bar{u})_o}{\tilde{\alpha}(C-1)}\right) = \frac{\alpha}{\tilde{\alpha}}\left(\frac{4(D\bar{u})_o}{N_{R_o}} + \frac{4\tilde{\alpha}(C-1)\coth\tilde{\alpha}}{N_{R_o}} + \frac{\alpha^{1/2}(C-1)^2(\coth^2\tilde{\alpha}-1)}{(2C\,N_{R_o})^{1/2}}\right) \quad (43)$$

$$\tilde{\alpha}^2 = \alpha^2 + \beta^2$$

## MODELS FOR THE GAS FLOW

In order to evaluate the conditions of neutral stability or the growth factor, expressions for $\hat{P}_I$, $\hat{P}_R$, and $\hat{T}_R$ are needed.

In accordance with the Kelvin-Helmholtz model (9) the air and water flows are uniform, a discontinuity in velocity is allowed at the interface, and the viscosities of the two fluids are zero. The compression of the streamlines at the crests is accompanied by a decrease in the gas pressure, while the spreading of the streamlines at the troughs causes an increase in the gas pressure. The Kelvin-Helmholtz model predicts a variation of the gas pressure over the wavy surface which is 180 deg. out of phase with the wave height:

$$\hat{P}_I = 0 \quad (45)$$

$$\hat{P}_R = -\rho_G (U_a - C)^2 \alpha \left(\frac{\alpha}{\tilde{\alpha}}\right)\hat{h} \quad (46)$$

Jeffreys (8) proposed that the separation of the gas flow on the back side of the waves causes a pressure variation in phase with the wave slope

$$\hat{P}_I = e\,\alpha\,\rho_G (U_a - C)^2 \frac{\alpha}{\tilde{\alpha}} h \quad (47)$$

in which the sheltering coefficient $e$ must be determined empirically. From observations of the generation of waves on a deep body of water, Jeffreys suggested that $e \cong 0.3$.

Miles and Benjamin derived expressions for the pressure and shear stress variations over a wavy surface by solving the Orr-Sommerfeld equations with an appropriate turbulent velocity profile. In their derivation it is assumed that the disturbances introduced into the gas flow by the waves do not interact with the turbulence in the gas. In the limit of large gas Reynolds number the viscous terms in the Orr-Sommerfeld equation are negligible over the whole flow field except for thin viscous layers at the critical point where the gas velocity equals the wave velocity and at the interface. In these viscous layers phase shifts occur in the fluctuating velocity and pressure. These phase shifts give rise to pressure components at the interface which are in phase with the wave slope without the occurrence of a separated flow.

For the range of wave velocities and wave lengths that are of interest in the present study the two viscous layers overlap, and the gas layer may be considered of infinite

TABLE 1. CONDITIONS AT INCEPTION OF TWO-DIMENSIONAL WAVES

| $N_R$ | $N_{RG}$ | $H$ (ft.) | $\mu\left(\frac{\text{lb. m}}{\text{hr.-ft.}}\right)$ | $\mu_G\left(\frac{\text{lb. m}}{\text{hr.-ft.}}\right)$ | $\rho_G\left(\frac{\text{lb. m}}{\text{cu. ft.}}\right)$ |
|---|---|---|---|---|---|
| Fluid—water; $\rho = 62.4 \frac{\text{lb. m}}{\text{cu. ft.}}$ | | | | | |
| 87 | 4,160 | 0.0060 | 2.18 | 0.0445 | 0.0705 |
| 135 | 3,100 | 0.0100 | 2.16 | 0.0446 | 0.0703 |
| 180 | 2,270 | 0.0132 | 2.13 | 0.0445 | 0.0702 |
| 222 | 1,470 | 0.0183 | 2.09 | 0.0445 | 0.0702 |
| 88 | 4,050 | 0.0062 | 2.25 | 0.0444 | 0.0714 |
| 125 | 3,640 | 0.0088 | 2.26 | 0.0444 | 0.0714 |
| 160 | 2,760 | 0.0116 | 2.26 | 0.0444 | 0.0714 |
| 198 | 2,200 | 0.0137 | 2.26 | 0.0444 | 0.0714 |
| 247 | 1,870 | 0.0161 | 2.24 | 0.0444 | 0.0714 |
| Fluid—(*G-I*); $\rho = 69.3 \frac{\text{lb. m}}{\text{cu. ft.}}$ | | | | | |
| 140 | 2,330 | 0.0210 | 9.56 | 0.0447 | 0.0694 |
| 127 | 2,590 | 0.0201 | 9.56 | 0.0447 | 0.0694 |
| 102 | 2,830 | 0.0181 | 9.51 | 0.0447 | 0.0694 |
| 89 | 3,060 | 0.0170 | 9.51 | 0.0447 | 0.0694 |
| 75 | 3,210 | 0.0160 | 9.44 | 0.0447 | 0.0694 |
| 61 | 3,600 | 0.0147 | 9.41 | 0.0447 | 0.0694 |
| Fluid—(*G-II*); $\rho = 73.0 \frac{\text{lb. m}}{\text{cu. ft.}}$ | | | | | |
| 46.9 | 3,650 | 0.0240 | 27.0 | 0.0447 | 0.0722 |
| 38.3 | 3,890 | 0.0222 | 27.0 | 0.0447 | 0.0722 |
| 30.2 | 4,170 | 0.0200 | 27.1 | 0.0447 | 0.0722 |
| 21.3 | 4,620 | 0.0173 | 27.2 | 0.0447 | 0.0722 |
| 15.2 | 5,030 | 0.0153 | 27.2 | 0.0447 | 0.0722 |

extent. Therefore, the method outlined by Miles (*17, 18*) for solving the Orr-Sommerfeld equation for the gas flow can be used. The Riccati equation defined by Miles was integrated numerically with velocity measurements obtained in the dry channel. Since the liquid has an average velocity, the measurements in the dry channel (with reference to a fixed boundary) were set equal to $U - 1$. By using Squire's transformation (*12*) the solution for two-dimensional disturbances given by Miles has been extended to include three-dimensional disturbances. The details of these calculations are presented in a thesis by one of the authors (*3*).

## MEASUREMENTS OF TRANSITION TO TWO-DIMENSIONAL WAVES

The conditions at the inception of two-dimensional waves are presented in Table 1. At the transitions to two- and three-dimensional waves it was found that $\hat{P}_R$ does not play an important role.

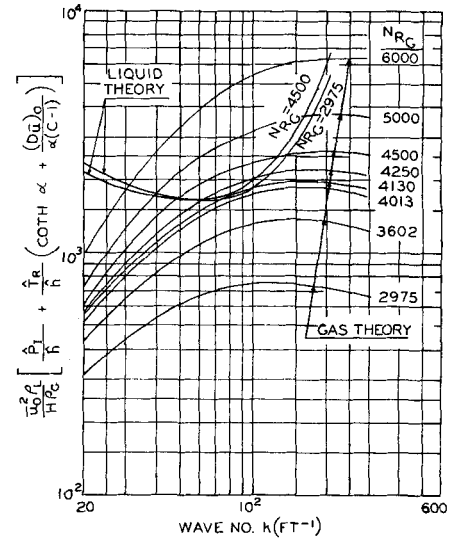


Fig. 2. Theoretical determination of wave inception conditions—G-I ($H$ = 0.0147 ft.).

The use of the Miles-Benjamin model or the Jaffreys sheltering hypothesis in conjunction with (40) predicts a critical value of the gas velocity above which two-dimensional waves will appear at the interface. In such a calculation the terms on the right side of (40), which are a measure of the energy dissipated by viscosity in the liquid film, are plotted vs. the wave number for a liquid of fixed height $H$ for several values of $N_{RG}$. The terms on the left side of (40), which are a measure of the energy fed to the liquid film by the gas flow, are plotted on the same graph for several values of $N_{RG}$. The gas Reynolds number at which a dissipation curve is tangent to an energy input curve is taken as the transition value, and the wave number at the point of tangency is used to calculate the wave length and wave velocity at transition, with Equation (39). This procedure is illustrated with the Miles-Benjamin model for the gas flow in Figure 2. A comparison of the experimental results and the predicted results with the models of Jeffreys and of Miles and Benjamin is presented in Table 2. Both models predict the effect of liquid Reynolds number on transition that has been observed in experiment (*5, 7*).

The observed values of $N_{RG}$ at wave inception are not exact, inasmuch as they depend somewhat on the judgment of the observer. It is not unreasonable to assign a margin of doubt of ± 10 to 20% to the observations. With this qualification, the agreement of Jeffreys' hypothesis, for $e$ = 0.3, and the Miles-Benjamin model with experiment must be considered good. Predictions of the wave length and wave velocity from both models are also in accord with visual estimates at wave inception, although

TABLE 2. COMPARISON OF EXPERIMENTAL RESULTS AT WAVE INCEPTION WITH THE PREDICTIONS OF THE JEFFREYS AND MILES-BENJAMIN THEORIES

| | Experimental results | | | | Jeffreys ($e$ = 0.30) | | | Miles-Benjamin | | |
|---|---|---|---|---|---|---|---|---|---|---|
| Fluid | $N_R$ | $N_{RG}$ | $C\left(\frac{\text{ft.}}{\text{sec.}}\right)$ | $\lambda_x$ (in.) | $N_{RG}$ | $C\left(\frac{\text{ft.}}{\text{sec.}}\right)$ | $\lambda_x$ (in.) | $N_{RG}$ | $C\left(\frac{\text{ft.}}{\text{sec.}}\right)$ | $\lambda_x$ (in.) |
| $H_2O$ | 88.0 | 4,056 | 1.2 | 0.9 | 3,300 | 1.00 | 0.331 | 4,500 | 0.92 | 0.75 |
| $H_2O$ | 161 | 2,760 | 1.1 | 1.2 | 2,300 | 0.95 | 0.514 | 3,100 | 1.02 | 0.85 |
| $H_2O$ | 247 | 1,870 | — | — | 1,900 | 0.97 | 0.674 | 2,500 | 1.22 | 0.94 |
| *G-I* | 140 | 2,330 | 1.2 | 1.2 | 2,800 | 1.11 | 0.933 | 3,300 | 1.65 | 1.16 |
| *G-I* | 61 | 3,600 | — | — | 3,300 | 0.93 | 0.692 | 4,100 | 1.06 | 0.94 |
| *G-II* | 47 | 3,650 | — | — | 3,900 | 1.04 | 1.063 | 4,300 | 1.21 | 1.16 |
| *G-II* | 21 | 4,620 | 1.2 | 1.2 | 4,700 | 0.89 | 0.871 | 5,900 | 1.12 | 0.96 |

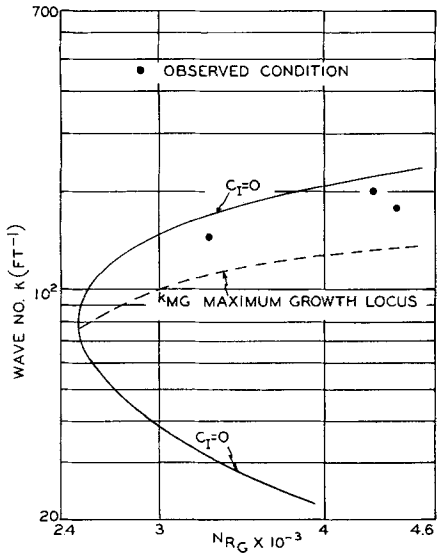


Fig. 3. Comparison of $k_{MG}$ with observed wave numbers—water (H = 0.0161 ft.).

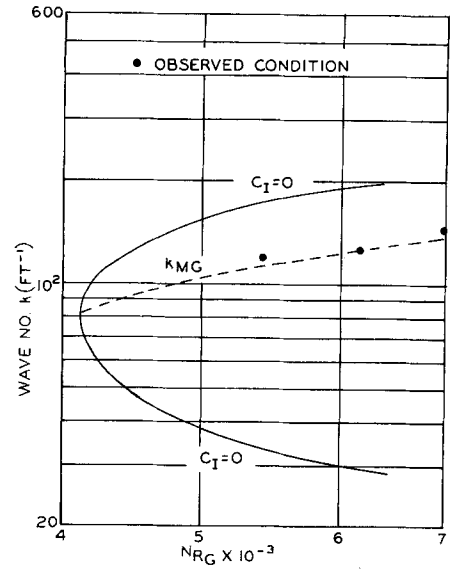


Fig. 4. Comparison of $k_{MG}$ with observed wave numbers—G-I (H = 0.0147 ft.).

the wave lengths for water predicted by Jeffreys' model appear to be too small.

Over the range of variables of interest in the present investigation, the Miles-Benjamin model indicates that pressure variations were playing a much more important role in generating waves than shear stress variations. In accordance with this model a plot of $\frac{1}{\rho_G}\frac{\hat{P}_I}{\hat{h}}$ at a fixed value of the gas flow rate shows the same behavior as shown in Figure 2 for the sum of the amplitudes of the pressure and shear stress fluctuations. This is quite different from the linear relation between $\hat{P}_I$ and $\alpha$ predicted by the Jeffreys model [see Equation (47)].

Neutral stability curves constructed from the Miles-Benjamin model of the gas flow are shown in Figures 3 and 4. Unstable disturbances lie within the region bounded by the envelope $C_I = 0$. The dotted line is the locus of the wave numbers $k_{MG}$ for which the growth factor given by (41) is a maximum. As indicated on these graphs, the wave numbers of two-dimensional waves observed above the critical gas velocity are in close agreement with calculated values of $k_{MG}$.

## MEASUREMENTS OF TRANSITION TO THREE-DIMENSIONAL WAVES

The Miles-Benjamin model was also applied to the problem of predicting $N_{RG}$, $C$, and $\lambda_x$ at the three-dimensional transition with (42) and (43). In these calculations $\lambda_x$ was taken equal to $\lambda_z$. As indicated in the description of the experiments, the definition of the transition to three-dimensional waves was somewhat arbitrary and corresponded to the appearance of waves whose dimensions in the $x$ and $z$ directions were approximately equal.

A comparison of the predicted and experimental results is given in Table 3. The theory shows the effect of liquid viscosity on the stability of two-dimensional waves noted in the experiments. In order to obtain the type of agreement shown in Table 3 with Jeffreys model the value of the sheltering coefficient must be reduced by an order of magnitude from that used to treat the transition to two-dimensional waves.

## CONCLUDING REMARKS

At sufficiently high air velocities two- and three-dimensional waves appear at the interface of a concurrent air-liquid flow. The disturbances in the velocity field in the air caused by these waves give rise to pressure and shear stress variations over the wavy surface. Pressure variations in phase with the wave slope and shear stress variations in phase with the wave height can transmit energy from the air flow to the liquid film. If the rate at which energy is transmitted to the waves by this mechanism is not larger than the rate of viscous dissipation in the liquid, the waves will decay.

Measurements of the air velocity at which two- and three-dimensional waves are initiated and of the wave lengths and wave velocities indicate that the linearized model proposed by Miles and Benjamin can be used to calculate the pressure and shear stress variations over waves of small amplitude. The agreement between calcu-

TABLE 3. COMPARISON OF EXPERIMENTAL RESULTS AT THE THREE-DIMENSIONAL TRANSITION WITH THE PREDICTIONS OF THE MILES-BENJAMIN THEORY

| | | | Experimental results | | | | | | Miles-Benjamin | | | |
|---|---|---|---|---|---|---|---|---|---|---|---|---|
| Fluid | $N_R$ | $N_{RG}$ | $H$ (in.) | $\mu$ (lb. m/hr.-ft.) | $\rho$ (lb. m/cu. ft.) | $\mu_G$ (lb. m/hr.-ft.) | $\rho_G$ (lb. m/cu. ft.) | $C$ (ft./sec.) | $\lambda_x$ (in.) | $N_{RG}$ | $C$ (ft./sec.) | $\lambda_x$ (in) |
| $H_2O$ | 590 | 4,100 | 0.199 | 2.30 | 62.4 | 0.0445 | 0.0707 | 1.03 | 0.39 | 3,200 | 1.09 | 0.56 |
| $H_2O$ | 400 | 4,200 | 0.158 | 2.20 | 62.4 | 0.0445 | 0.0705 | 1.01 | 0.49 | 3,800 | 1.02 | 0.48 |
| $H_2O$ | 250 | 4,400 | 0.112 | 2.24 | 62.4 | 0.0445 | 0.0704 | 0.90 | 0.50 | 4,700 | 0.94 | 0.46 |
| *G-I* | 150 | 8,400 | 0.181 | 9.09 | 69.2 | 0.0445 | 0.0697 | 1.27 | 0.47 | 6,100 | 1.07 | 0.53 |
| *G-I* | 90 | 9,000 | 0.124 | 9.57 | 69.3 | 0.0445 | 0.0697 | 1.20 | 0.44 | 8,000 | 1.09 | 0.48 |
| *G-I* | 61 | 9,600 | 0.082 | 9.45 | 69.3 | 0.0445 | 0.0697 | 0.95 | 0.40 | 10,200 | 0.97 | 0.38 |

lations based on this model and experiment is quite good, since no empirical constants are used. Since the Jeffreys model requires that an empirical constant be evaluated from the measurements, and since the Miles-Benjamin model appears to do a better job of explaining all of the measurements, it is felt that the Jeffreys hypothesis is not applicable to the measurements reported in this paper.

However, for waves of larger height than those discussed in this paper, separation of the air flow might occur, and Jeffreys' model might be more appropriate than the model of Miles and Benjamin based on no separation.

Finally, it should be emphasized that the mechanism suggested in this paper is not the only possible mechanism for the generation of waves. Experiments (2) performed on the concurrent flow of two liquids indicate that a resonance mechanism of the type suggested by Phillips is responsible for the first waves which are observed.

It would appear that there are a number of possible mechanisms by which waves can be generated. The task is to determine under which conditions these different mechanisms are operative.


## ACKNOWLEDGMENT

This work has been supported by the National Science Foundation under Grant G-14788.


## NOTATION

$B$ = channel height
$C$ = wave velocity
$D$ = $d/dy$
$N_F$ = Froude number = $\bar{u}_o/\sqrt{gH}$
$g$ = acceleration of gravity
$H$ = average height of the liquid
$h$ = instantaneous height of the liquid
$i$ = $\sqrt{-1}$
$k$ = dimensional wave number = $2\pi/\lambda$
$m$ = $\sqrt{-i}$
$P$ = pressure in the gas at the interface
$p$ = pressure in the liquid
$N_R$ = Reynolds number based on the mixed average velocity and the height of the liquid film
$N_{R_o}$ = Reynolds number based on the average velocity at the interface and the height of the liquid film
$N_{R_G}$ = Reynolds number based on the bulk average gas velocity and the height of the gas layer
$s^2$ = $-i\,(C-1)/C$
$t$ = time
$T$ = shear stress of the gas on the liquid surface
$U$ = velocity of the gas in the $x$ direction
$u$ = velocity of the liquid in the $x$ direction
$v$ = velocity of the liquid in the $y$ direction
$N_W$ = Weber number = $6/\rho\,\bar{u}_o^2\,H$
$w$ = velocity of the liquid in the $z$ direction
$x$ = coordinate in the direction of mean flow
$y$ = height coordinate
$z$ = width coordinate

### Greek Letters

$\alpha$ = nondimensional wave number in $x$ direction = $\dfrac{2\pi H}{\lambda_x}$
$\tilde{\alpha}$ = $(\alpha^2+\beta^2)^{1/2}$
$\beta$ = wave number in the z direction = $\dfrac{2\pi H}{\lambda_z}$
$\eta$ = $(1+y)\mathcal{R}^{1/3}$
$\lambda_x$ = wave length in $x$ direction
$\lambda_z$ = wave length in $z$ direction
$\mu$ = viscosity of the liquid
$\nu$ = kinematic viscosity of the liquid
$\xi$ = $y\,\mathcal{R}^{1/3}$
$\rho$ = density of the liquid
$\rho_G$ = density of the gas
$\sigma$ = surface tension
$\tau_{ij}$ = stress in the liquid in the $j$ direction on a plane normal to the $i$ coordinate

### Script Letters

$\mathcal{L}$ = $D^2\bar{u}/C\,\alpha^2$
$\mathcal{R}$ = $\sigma\,C\,R_o$
$\hat{\mathcal{S}}$ = $\dfrac{\alpha}{\tilde{\alpha}}\left(\hat{T}_{x'}+\dfrac{\beta}{\alpha}\hat{T}_{z'}\right)$

### Subscripts

$a$ = bulk average
$G$ = gas parameter
$I$ = imaginary part
$o$ = at interface
$R$ = real part
$v$ = viscous solution
$w$ = at wall
$x,x'$ = $x$ direction or $x'$ direction
$y,y'$ = $y$ direction or $y'$ direction
$z,z'$ = $z$ direction or $z'$ direction

### Superscripts

$'$ = fluctuating quantity
$\Lambda$ = amplitude functions described by Equations (6)
$\bar{\ }$ = time average
$\tilde{\ }$ = transformed variables for three-dimensional disturbances

## LITERATURE CITED


1. Benjamin, T. B., *J. Fluid Mech.*, **6**, 161 (1959).
2. Charles, M. E., Ph.D. thesis, University of Alberta, Canada (1963).
3. Cohen, L. S., Ph.D. thesis, University of Illinois, Urbana, Illinois (1964).
4. Feldman, Saul, *J. Fluid Mech.*, **2**, 343 (1957).
5. Hanratty, T. J., and J. M. Engen, *A.I.Ch.E. Journal*, **3**, 299 (1957).
6. Hanratty, T. J., and Arnold Hershman, *ibid.*, **7**, 488 (1961).
7. Hershman, Arnold, Ph.D. thesis, University of Illinois, Urbana, Illinois (1960).
8. Jeffreys, H., *Proc. Royal Soc.*, **A107**, 189 (1925).
9. Lamb, H., "Hydrodynamics," 6 ed., Dover, New York (1945).
10. Lilleleht, L. U., Ph.D. thesis, University of Illinois, Urbana, Illinois (1962).
11. Lilleleht, L. U., and T. J. Hanratty, *J. Fluid Mech.*, **11**, 65 (1961).
12. Lin, C. C., "The Theory of Hydrodynamic Stability," Cambridge Univ. Pres, London, England (1955).
13. Lock, R. C., *Proc. Camb. Phil. Soc.*, **50**, 105 (1954).
14. Miles, J. W., *J. Fluid Mech.*, **3**, 185 (1957).
15. *Ibid.*, **6**, 568 (1959).
16. *Ibid.*, p. 583.
17. *Ibid.*, **13**, 433 (1962).
18. *Ibid.*, p. 427.
19. *Ibid.*, **8**, 593 (1960).
20. Motzfeld, H., *Z. Angew. Math. Mech.*, **17**, 193 (1937).
21. Phillips, O. M., *J. Fluid Mech.*, **2**, 417 (1957).
22. Stanton, T. E., D. Marshall, and R. Houghton, *Proc. Roy. Soc.* **A137**, 283 (1932).
23. Ursell, F., "Surveys in Mechanics," pp. 216-249, Cambridge Press, London, England (1956).



*Manuscript received May 15, 1964; revision received September 9, 1964; revision recevied September 11, 1964.*